IEEE Access
Multidisciplinary | Rapid Review | Open Access Journal

Received March 31, 2021, accepted April 15, 2021, date of publication May 21, 2021, date of current version June 1, 2021.

Digital Object Identifier 10.1109/ACCESS.2021.3082766

A Channel-Aware Adaptive Modem for Underwater Acoustic Communications

STEFANO MANGIONE[1,2,3], (Member, IEEE), GIOVANNI ETTORE GALIOTO[1,3], DANIELE CROCE[1,2,3,4], ILENIA TINNIRELLO[1,2,3], AND CHIARA PETRIOLI[3,4], (Fellow, IEEE)

[1]Department of Engineering, University of Palermo, 90133 Palermo, Italy
[2]Consorzio Nazionale Interuniversitario per le Telecomunicazioni (CNIT), 43124 Parma, Italy
[3]WSense Srl, 00198 Rome, Italy
[4]Department of Computer Science, University of Rome La Sapienza, 00185 Rome, Italy

Corresponding author: Daniele Croce (daniele.croce@unipa.it)

This work was supported in part by the Italian Ministry of Defense through the framework of the National Plan of Military Research by the General Secretariat of Defense and the National Directorate of Armaments under Grant a2017.132. The work of Stefano Mangione, Giovanni Ettore Galioto, Daniele Croce, and Ilenia Tinnirello was supported in part by WSense Srl.

ABSTRACT Acoustic underwater channels are very challenging, because of limited bandwidth, long propagation delays, extended multipath, severe attenuation, rapid time variation and large Doppler shifts. A plethora of underwater communication techniques have been developed for dealing with such a complexity, mostly tailoring specific applications scenarios which can not be considered as one-size-fits-all solutions. Indeed, the design of environment-specific solutions is especially critical for modulations with high spectral efficiency, which are very sensitive to channel characteristics. In this paper, we design and implement a software-defined modem able to dynamically estimate the acoustic channel conditions, tune the parameters of a OFDM modulator as a function of the environment, or switch to a more robust JANUS/FSK modulator in case of harsh propagation conditions. The temporal variability of the channel behavior is summarized in terms of maximum delay spread and Doppler spread. We present a very efficient solution for deriving these parameters and discuss the limit conditions under which the OFDM modulator can work. In such scenarios, we also calibrate the prefix length and the number of sub-carriers for limiting the inter-symbol interference and signal distortions due to the Doppler effect. We validate our estimation and adaptation techniques by using both a custom-made simulator for time-varying underwater channels and the well-known Watermark simulator, as well as real in field experiments. Our results show that, for many practical cases, a dynamic adjustment of the prefix length and number of sub-carriers may enable the utilization of OFDM modulations in underwater communications, while in harsher environments JANUS can be used as a fall-back modulation.

INDEX TERMS Channel estimation, JANUS, modems, OFDM, software radio, underwater communication, watermark.

I. INTRODUCTION

The past three decades have seen a growing interest in underwater acoustic communications, with the rise of new underwater applications such as remote control in the off-shore oil industry, pollution monitoring in environmental systems, collection of scientific data from ocean-bottom stations, disaster detection and early warning, national security and defense, e.g. intrusion detection and underwater surveillance. Indeed, the research of new underwater wireless communication techniques has played an important role in the exploration of oceans and other aquatic environments.

Underwater wireless communications are very challenging, because the acoustic channel is characterized by limited bandwidth, severe attenuation (increasing with the signal frequency), long propagation delays due to the sound speed (about 1500 m/s), frequency dispersion, and time-varying multipath [1]. Sound speed profiles due to the heterogeneous water salinity increases the number of potential reflections, while surface waves, internal turbulence, fluctuations in the sound speed at different depths, and other small-scale phenomena contribute to random signal variations, which may

The associate editor coordinating the review of this manuscript and approving it for publication was Qiong Wu.

strongly vary from one environment to another (e.g. from shallow waters, to pools or port environments).

The large diversity of underwater wireless scenarios and environments is reflected in different varieties of modems and architectures which are present in literature and on the market. Most of the approaches that have been proposed can be roughly divided into two categories: i) very robust, low rate modems reaching a rate in the order of hundreds of bits/s, exploiting long-lasting symbols and various types of spread spectrum modulations; ii) high speed modems for short/medium distance connections (tens to hundreds of meters), employing for example OFDM modulations and high frequency acoustic transducers operating in ultra-sonic bands (around 100 kHz or above), reaching nominal data rates of hundreds of kbit/s (e.g. [2]).

The first category of solutions work by using symbols whose duration is higher than the propagation delays of the most powerful reflected path. In some cases, gap intervals are added between consecutive symbols, in order to allow the extinction of the symbol reflection before transmitting a new symbol. Moreover, consecutive symbols can be transmitted by hopping from one carrier frequency to another, as done in JANUS [3], for leaving signal reflections in a sub-band different from the current used one and avoiding inter-symbol interference (ISI). Other spread-spectrum solutions devised to work in challenging environments exploit chirp-based modulations, such as the Sweep Spread Carrier (S2C) modulation used by Evologics modems [4]. The second category of solutions address the problem of inter-symbol interference and scarce bandwidth availability by using multi-carrier modulations, trying to achieve higher spectral efficiency. However, applying multi-carrier modulations such as OFDM to acoustic channels is a challenging task, because of its sensitivity to frequency offsets due to motion, currents, and clock stability of the nodes. In particular, because of the low speed of sound, motion-induced Doppler effects due to waves and node's drifting may result in critical problems, such as non-uniform frequency shifts across the signal bandwidth and inter-carrier interference (ICI). Different solutions have been proposed for dealing with the Doppler effect, by estimating and compensating at the receiver the time compression or dilatation effect due to the Doppler on a per-packet (e.g. [5]) or per-symbol basis (e.g. [6]). However, most of these approaches significantly reduce the data rate or increase the computational complexity, and therefore the power consumption, of the receiver.

In this work, we investigate on a simple strategy for coping with the Doppler effect: rather than implementing a complete Doppler compensation technique at the receiver, we periodically estimate the channel spreading parameters and dynamically adjust the OFDM parameters in order to be robust under the maximum expected Doppler shift and multipath delay. While usual OFDM adaptations work on the choice of constellations with different cardinality, in our case we adapt the number of sub-carriers to be deployed over the channel bandwidth and the length of the cyclic prefix. The basic assumption for our design is that, for many applications, the underwater channel is good enough to allow the set-up of an OFDM-link and an opportunistic (periodic) calibration of the OFDM modulation parameters is possible in scenarios with mild temporal variability of environmental parameters due for example to particular weather conditions, temperature and salinity of the water, as well as the site-specific propagation environment.

To demonstrate the effectiveness of our approach, we designed a low-complexity estimation technique for time-varying channels, based on the transmission of pre-defined linear modulated frequency chirps, and an intelligent module for tuning the OFDM parameters as a function of the channel spreading estimates. The modules have been validated in different simulation platforms for underwater communications and in real experiments at sea. For the experimental validation, we exploited a software-defined-modem developed by our research group [7], which has been extended for running: i) the intelligent module for channel-adaptation, ii) an OFDM modulator exposing a configuration interface to the intelligent module; iii) a JANUS modulator, providing a robust feedback (and back-up) channel for notifying the channel spreading estimates to the transmitter. The main contributions introduced in this paper are therefore:

- a low complexity channel spreading estimation method, exploited in the software defined modem to adjust the modulation parameters (possibly switching modulation), to optimize both speed and robustness of the communications;
- an enhanced OFDM scheme with decision feedback receiver, which is able to compensate channel variations within the OFDM transmission;
- a thorough validation of the proposed techniques, based on both numerical simulations and in-field experiments.

The rest of the paper is organized as follows: after a brief literature review about OFDM schemes for underwater channels and relevant experimentation platforms (section II), we present the characteristics of the proposed system architecture in section III and the channel estimation method in section IV. We analyze some reference underwater scenarios (both in simulation and real experiments) in section V. Then, in sections VI and VII we assess the performance, respectively, of the OFDM and JANUS modulators integrated in our system. Finally, conclusions are drawn in section VIII.

II. RELATED WORK

A. OFDM SOLUTIONS FOR UNDERWATER CHANNELS

In the last decade, multi-carrier modulations, such as OFDM, have emerged as a promising solution for underwater communications [8], because of their robustness to channels which exhibit long delay spreads and frequency selectivity. However, these modulation solutions also have to specifically address the significant Doppler effect which affects underwater acoustic channels. Indeed, even for limited node

motion and good clock stability, the low speed of sound and the fact that the acoustic bandwidth is not negligible with respect to the center frequency, make the Doppler effects critical. Different solutions have been proposed for addressing this problem, by designing receivers with some adaptation capabilities [9]. Adaptions can involve traditional approaches based on the choice of per-carrier constellations, such as the first scheme demonstrated in [10] or the On-Off keying solution for non-coherent receivers presented in [11], as well as adaptive coding techniques [12]. However, to achieve high reliability under general propagation conditions, Doppler estimation and compensation techniques are often required [13]. Different assumptions on the channel conditions lead to different complexity of the receivers. When the channel can be assumed quasi-static or with uniform Doppler shifts, an average Doppler scaling factor can be estimated with a given resolution by correlating special preamble signals with different distorted versions of the same known preamble [14], [15]. Recent proposals have also addressed the case when the Doppler scaling cannot be assumed constant for the whole data packet. Indeed, with fast-varying movements, the Doppler estimation needs to be updated more frequently, even for each data symbol [6]. Per-symbol estimates are usually based on the evaluation of the cross-ambiguity function [16] which is a computationally intense task, and more recently multi-branch auto-correlation methods have been devised in order to lower its complexity [17].

Differently from these approaches, our solution does not try to estimate and correct the exact Doppler scale over time, but it estimates the worst expected Doppler shift for tuning the OFDM parameters, and compensates symbol by symbol the average clock drift. This design choice leads to a solution with a complexity much lower than [17], which works well under the assumption that, even if the instantaneous Doppler shift and multi-path Delay parameters can vary relatively fast, the overall channel spreading parameters will be slowly time-varying.

B. EXPERIMENTAL PLATFORMS FOR UNDERWATER OFDM SCHEMES

Nowadays, most commercial acoustic modems rely on fixed hardware designs and proprietary protocol solutions, designed for providing low-rate robust links and exposing a few configurable parameters. Only some recent modems support high-rate communications (up to hundreds kbits/s), and the possibility to switch among multiple pre-defined modulation schemes [18], [19]. Some models also permit the transmission of programmable waveforms, thanks to an hardware interface devised to load (and to read) the digital samples of a base-band modulated signal [20]. However, in this configuration, the base-band processing is performed in external devices e.g. using external libraries or software stacks (e.g. [21]).

Because of the limited flexibility of commercial solutions, most of the OFDM schemes designed for underwater environments have been experimentally validated by means of expensive research prototypes [22]. For example, in [23], an OFDM base-band implementation based on a DSP board is presented, with a single-core CPU running at 1GHz, able to support modulations from QPSK up to 64-QAM and working with multiple transmitters. A complete implementation, including an embedded computer for high-layer processing, a DSP board for base-band processing and an FPGA board for pass-band processing is described in [24]. Different OFDM variants, which include incoherent and coherent OFDM schemes, are available for this implementation as DSP pre-configured modules.

A complete software-defined-acoustic-modem (SDAM) able to work at high-data rates is described in [2]. The model can seamlessly switch between different communication technologies such as OFDM and spread-spectrum modulations. At high rates, it can support up to 260 kbps in real-time over a link of 200 m, by adapting the modulation order and coding rate as a function of the channel conditions. For supporting this rate, the platform makes use of expensive hardware, including the USRP N210 (FPGA-based software defined radios), and a powerful PC for running the GNU Radio software.

Differently from [2] and other previous work, where expensive hardware is required and where the adaptation of the modulation parameters is done solely according to reception errors, in this paper we propose a software architecture for implementing a OFDM adaptive system, which runs on a simple Red Pitaya board, an open-source hardware project that includes a dual-core ARM CPU and a high performance FPGA by Xilinx. Rather than using the GNU Radio libraries, we exploited the liquid-dsp [30] signal processing library, written in C, for improving the code efficiency. Moreover, we extended the experimental platform presented in [7] for automatically tuning the modulation parameters (e.g. number of OFDM sub-carriers and cyclic prefix length), as a function of the estimated channel conditions. This capability is very different from previous OFDM modems, such as [2], where only reception failures are considered in the feedback channel. Note also that our modem works with a central frequency lower than the one used in [2], and with a much smaller bandwidth (namely, 16 kHz vs. 96 kHz). Alternative solutions working on carriers at lower frequencies usually adopt low-rate modulations for supporting robust links. For example, the compact Micro-Modem [25], [26] implements two modulation schemes: frequency-hopping frequency-shift keying (FH-FSK), reaching a data rate of 80 bit/s, and phase shift keying (PSK) obtaining data rates from 300 to 5000 bit/s. The SeaModem described in [27] is another underwater acoustic modem that features a M-FSK (2, 4 and 8 tones) modulation with frequency band from 25 to 35 kHz and data rates of 750, 1500 and 2250 bit/s depending on the number of tones used. A more advanced configuration of the modem is presented in [28], where the JANUS FH-BFSK scheme was added to the native M-FSK modulation.

Table 1 summarizes the main characteristics of the above mentioned approaches, comparing them with the approach

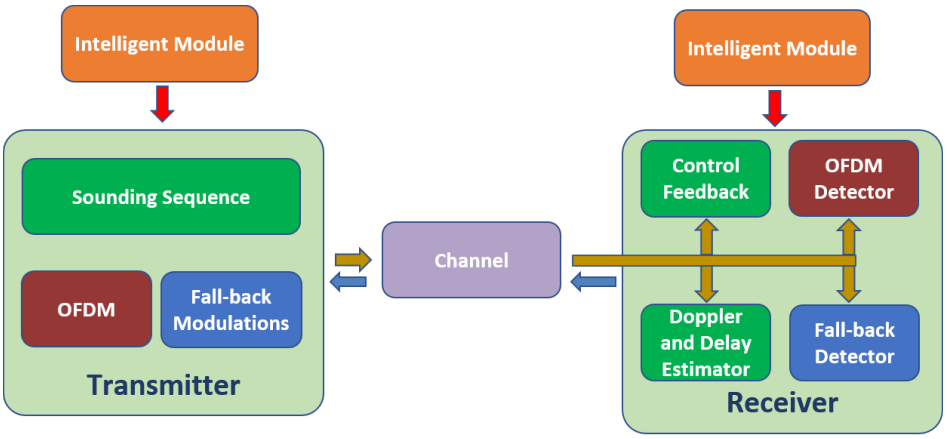

FIGURE 1. High-level block scheme of the proposed communication system.

TABLE 1. Comparison between relevant previous works and the proposed modem.

Modem	Freq. band	Modulation	Max Rate
SEANet-G3 [2]	76 – 174 kHz	ZP-OFDM	208 kb/s
UNET-2 [19], [24]	18 – 36 kHz	OFDM	9 kb/s
UCONN [23]	9 – 15 kHz	MIMO OFDM	6.4 kb/s
Micro-Modem [25], [26]	3 – 30 kHz	FH-FSK, PSK	5 kb/s
EvoLogics WiSE [18]	18 – 34 kHz 48 – 78 kHz	S2C	13.9 kb/s 31.2 kb/s
SeaModem [27]	25 – 35 kHz	M-FSK, JANUS	2.25 kb/s
Proposed modem	14 – 30 kHz 18 – 34 kHz	OFDM, JANUS	20 kb/s

proposed in this paper in terms of frequency band, modulation format and maximum achievable data rate. A more comprehensive comparison on underwater modems (including power consumption data) can be found in [29]. In the band around [18 – 34] kHz, our solution achieves data rates comparable or higher than the ones of [18] in presence of good channel conditions. However, we want to remark that our main goal is not maximizing such a data rate in absolute terms, but rather optimizing the data rate achievable for specific channel conditions, thanks to the dynamic tuning of OFDM parameters.

III. HIGH-LEVEL SYSTEM DESIGN

Figure 1 summarizes the high-level design of the envisioned adaptive modem. The design has been motivated by the need of addressing very heterogeneous propagation scenarios: i) the case of *quasi-static or underspread channels*, for which modulations with high spectral efficiencies can be considered; ii) the case of *harsh or overspread channels*, for which only robust (low-rate) modulations can achieve a non-null transmission capacity. To cope with this heterogeneity, different forms of adaptations are supported. First, the modem is equipped with two different *software* transceivers: an OFDM modulator, able to optimize the usage of the transmission bandwidth for benign channels, and a fall-back modulator, providing a robust back-up link in case of difficult channel conditions. Second, the OFDM modulator can change the number of sub-carriers and the length of the cyclic prefix, in order to respond to the variability of multipath and Doppler effects, which may be encountered in different sites and applications.

Decisions on the selection of the best modulator, as well as on the tuning of the modulator parameters, are taken by an intelligent module after estimating the operating conditions of the system. These conditions are summarized in terms of channel spreading parameters, i.e. analysis of the variability of signal interference and distortions due to multi-path reflections and Doppler effects. The analysis is performed on the receiver side on the basis of special sounding sequences transmitted at the system start-up or any time the intelligent module needs an update (e.g. when the communication link is experiencing high error rates). The fall-back modulator is used as a feedback channel from the receiver to the transmitter for sending back the results of the analysis.

A. INTELLIGENT MODULE

Generally, in OFDM communications the maximum symbol duration must be related to the coherence time of the channel (inversely proportional to the Doppler spread), which indicates the period of time the channel can be considered as stationary. Increasing the number of sub-carriers, improves the spectral efficiency and thus the overall bit rate of the transmission. However, if the number of subcarriers is too high, channel variations might cause errors in the demodulation, increasing the Bit-Error-Rate (BER). On the other hand, the duration of the cyclic prefix must be related to the delay spread of the channel, which measures the time duration of the multipath. The cyclic prefix must be large enough so that any interference phenomena due to multipath affects the next symbol only on the cyclic prefix, leaving the remaining part of the symbol unaffected.

Decisions of the intelligent module are based on the characterization of the channel behavior in terms of maximum

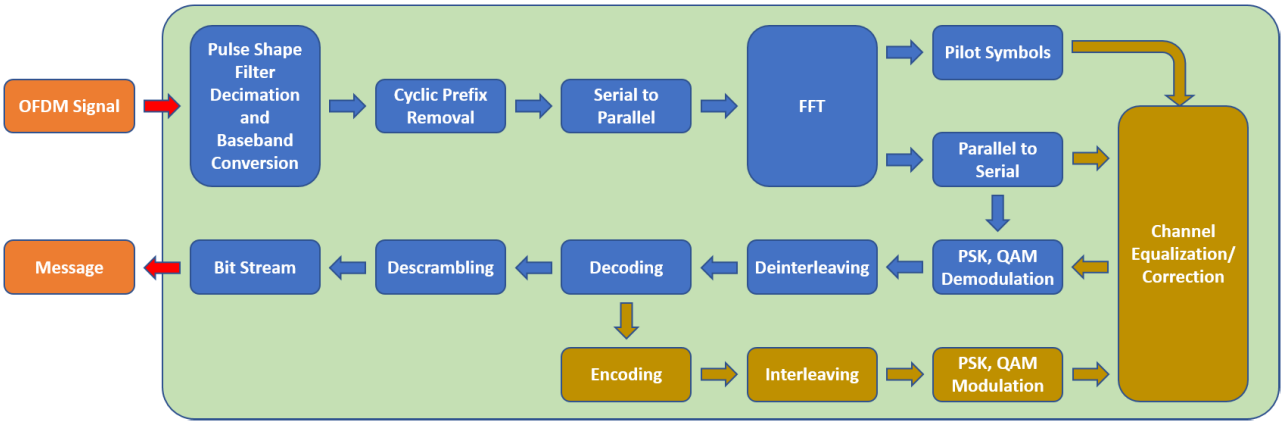

FIGURE 2. Block scheme of the OFDM receiver. The traditional receiver scheme is enhanced with re-encoding and channel correction blocks in yellow.

observable Doppler shift and multipath delay. These parameters are represented by the Doppler spread and Delay spread parameters, whose estimation is detailed in the next section. Assuming that these parameters are available, the intelligent module computes the following bounds:

$$N_{CP} \geq \frac{\text{Delay spread}}{T_s} \tag{1}$$

$$N + N_{CP} \leq \frac{0.08}{\text{Doppler spread} \cdot T_s} \tag{2}$$

where T_s is the signaling period and the 0.08 term is derived by allowing (approximately) an 8% variation of the channel impulse response. Note that, when the Delay spread is too large compared to the channel coherence time, the above inequalities would lead to an unfeasible system with $N < 0$. In this case, OFDM cannot be used with a arbitrarily low BER since loss of orthogonality is unavoidable. Therefore, the intelligent module selects the fall-back modulator. Otherwise, OFDM is chosen and configured with the best possible transmission rate.

B. OFDM MODEM

We implemented a Cyclic-Prefixed OFDM modulation with the following tunable parameters:

- N: number of subcarriers
- N_{CP}: length of the cyclic prefix (in number of samples)
- α_p: roll-off factor of the raised cosine filter
- L_p: length of the raised cosine filter (in signaling periods)

Data frames include a preamble symbol, which exploits all usable subcarriers, except the null ones, while four fixed pilot subcarriers are used for phase correction in each subsequent data symbol. Phase-tracking pilot subcarriers are equally spaced throughout the band, according to the so called Comb-Type configuration. Figure 2 shows the block scheme of the OFDM receiver, which performs channel frequency response estimation on a symbol-by-symbol basis, by using decision-feedback detection (rather than estimating the channel with the preamble only, which is only feasible on quasi-static channels). The decision feedback receiver is similar to the one proposed in [31], that we decided to employ here in order to be able to track channel frequency response variations during the data frame. In order to detect the reception of a packet, the receiver operation starts with a self-correlation threshold search on the received signal. Once an incoming signal is detected, the modem performs the initial channel estimation by comparing the received symbol with the known preamble waveform.

This initial estimate is used to detect the following OFDM symbol, which carries a Forward Error Correction (FEC) encoded data segment. The FEC we employed is a block channel encoder, so that each OFDM symbol carries its own codeword which can be decoded independently of the codewords carried by the preceding or following OFDM symbols.

Each decoded data segment, is re-encoded with the FEC, and re-mapped to the corresponding constellation points in order to create a reference symbol which is then used to re-estimate or update the estimated channel frequency response of the channel. Indeed, the regenerated signal represents the symbol originally transmitted by the sender and can be used as a reference to estimate the channel using all available subcarriers by comparing the constellation points actually received with the regenerated ones. The corrected channel is finally used to equalize the reception of the next symbol and, recursively, the channel equalization is updated at every symbol received. This decision feedback mechanism allows to track channel changes on a symbol-by-symbol basis and allows for reliable operation on fast-varying frequency selective fading channels. It is worth noting that this strategy also allows to efficiently synthesize the time-domain signal which can be used to track possible Doppler scale variations.

C. FALL-BACK MODEM

Different approaches have been envisioned for providing robustness in underwater channels, such as long symbol times, inter-symbol gaps and spread-spectrum techniques.

Long symbol times or gap intervals guarantee the extinction of the symbol reflections before transmitting a new symbol, while spread-spectrum solutions, including frequency hopping, increase robustness to noise and inter-symbol interference. Among the different options for supporting the fall-back modem, in our implementation we chose the JANUS standard [3], in order to facilitate interoperability. In particular, we have integrated the WSense and Rome La Sapienza implementation of JANUS which complies with NATO STANAG standard [3], [32].

JANUS adopts a Frequency-Hopped (FH) Binary Frequency Shift Keying (BFSK) modulation scheme because of its robustness in underwater propagation and its implementation simplicity. In this scheme, each bit is mapped into a pair of tones, selected among 13 possible equidistant pairs in the range from 9440 to 13600 Hz. At each symbol time, a new pair of tones is used for modulation, following a pseudo-random sequence, in order to avoid in-band inter-symbol interference. The data frame structure follows the basic JANUS package, consisting of an acoustic waveform that encodes 64 bits of information, preceded by a fixed synchronization sequence of 32 symbols. Furthermore, at the end of the basic package, an additional Data Cargo payload can be added. The robustness to temporal and frequency fading is provided by the convolutional coding with 2:1 redundancy, followed by interleaving. Error checking is performed using 8-bit CRC (Cyclic Redundancy Check).

IV. ESTIMATION OF CHANNEL SPREADING PARAMETERS

A key element of our system is represented by the estimation of the channel behavior. For channel behavior we do not mean the channel impulse response at a given time, but rather a simple characterization of the variability of this response as time varies.

A. CHANNEL ESTIMATION FOR TIME-INVARIANT CHANNELS

We start by deriving a channel estimation strategy for a linear time-invariant channel whose input-output relation may be written as

$$y_n = \sum_k h_k x_{n-k} + w_n \tag{3}$$

where x_n and y_n are respectively the input and output sequences, h_n is the channel impulse response and w_n is an equivalent noise including actual interference or noise and other measurement errors.

With the assumption that $h_k = 0$ for $k < 0 \vee k > L$, this equation may be rewritten in matrix form as follows:

$$y_n = \begin{bmatrix} x_n & x_{n-1} & x_{n-2} & \cdots & x_{n-L} \end{bmatrix} \begin{bmatrix} h_0 \\ h_1 \\ h_2 \\ \vdots \\ h_L \end{bmatrix} + w_n. \tag{4}$$

A subsequence $(y_n, y_{n+1}, y_{n+2}, \ldots, y_{n+M})$ of channel outputs can be used to build the following linear system:

$$\begin{bmatrix} y_n \\ y_{n+1} \\ y_{n+2} \\ \vdots \\ y_{n+M} \end{bmatrix} = \begin{bmatrix} x_n & x_{n-1} & x_{n-2} & \cdots & x_{n-L} \\ x_{n+1} & x_n & x_{n-1} & \cdots & x_{n+1-L} \\ x_{n+2} & x_{n+1} & x_n & \cdots & x_{n+2-L} \\ \vdots & \vdots & \vdots & \ddots & \vdots \\ x_{n+M} & x_{n+M-1} & x_{n+M-2} & \cdots & x_{n+M-L} \end{bmatrix} \begin{bmatrix} h_0 \\ h_1 \\ h_2 \\ \vdots \\ h_L \end{bmatrix} + \begin{bmatrix} w_n \\ w_{n+1} \\ w_{n+2} \\ \vdots \\ w_{n+M} \end{bmatrix} \tag{5}$$

or, in matrix form,

$$\mathbf{y} = \mathbf{X}\mathbf{h} + \mathbf{w}. \tag{6}$$

Provided the matrix $\mathbf{X}$ is known, this system can be solved for a Least Squares estimate of the channel impulse response $\mathbf{h}$ as follows:

$$\hat{\mathbf{h}} = \mathbf{X}^{+}\mathbf{y} \tag{7}$$

where $\mathbf{X}^{+}$ is the Moore-Penrose pseudoinverse of $\mathbf{X}$.

We assume that $\mathbf{X}$ is known since its components are given by samples of the transmitted sequence, called *sounding sequence*. When $M = L$, this matrix is square, and the sounding sequence may be chosen in such a way to optimize the channel estimation error and/or simplify the computation. Common choices for x_n are pseudo-noise or linear frequency modulated signals as reported in [33].

B. SOUNDING SEQUENCES FOR CHANNEL PROBING

We are interested in a channel estimation strategy which can be executed in real-time by a low-cost platform. This requires low-complexity methods for: (i) detection of the presence of the transmitted sounding signal while unsynchronized, (ii) estimation of the channel impulse response, (iii) estimation of the channel spreading features we are interested in.

For reasons that will be clear shortly, we choose to employ a sounding sequence signal made of periodic repetitions of chirp-like signals. The baseband signal we employ is the following:

$$s(t) = \sum_{l=0}^{N_c} \sum_{n=0}^{N_s-1} c_n p(t - (n + lN_s)T_s) \tag{8}$$

where N_s is the number of samples used and $N_c + 1$ is the number of repetitions of the sequence $c_n = \exp(-\jmath\pi(n - n^2/N_s))$. The signaling period T_s is the inverse of the channel

bandwidth, while $p(t)$ is a root-raised-cosine signaling pulse which is zero-ISI Nyquist at rate $1/T_s$.

The received baseband signal will be given by (time-varying) convolution between $s(t)$ and the channel impulse response. The received sequence y_n is obtained at the receiver side by matched filtering of the received signal, and sampling at rate $1/T_s$, i.e. by projection of the received signal onto $p(t - nT_s)$:

$$y_n = \langle r(t), p(t - nT_s) \rangle \tag{9}$$

where $r(t) = \int s(\tau)h(t,\tau)d\tau \cong \int s(\tau)h(t-\tau)d\tau$, $h(t,\tau)$ is the time-varying channel impulse response (i.e. channel output for an input impulse at time τ) and $h(t)$ is the time-invariant estimate we can measure at a given time. Note that a Carrier Frequency Offset or phase drift in the received signal will appear as a time-varying common phase term in the estimated channel impulse response.

C. LOW COMPLEXITY CHANNEL ESTIMATION

If the channel coherence time is not too short, i.e. smaller than the probing signal duration, the receiver can detect its presence by simple correlation of two consecutive N_s-samples subsequences. Specifically, following the Schwarz inequality, the receiver has to compute their inner product and compare it to the square root of the product of their energies.

The parameter N_s determines both the period of the probing signal and the channel-impulse response sampling rate. We obtain a channel estimate every N_sT_s received samples, and this means that the measurable Doppler range is $\pm 1/2N_sT_s$, while the maximum measurable delay spread is limited by N_sT_s (assuming that there is a direct path of maximum amplitude, otherwise it must be reduced by $1/2$). Therefore, N_s should be chosen the smallest possible without incurring in time-aliasing issues and can be adjusted iteratively by means of a feedback channel as devised e.g. in [2].

An estimate is obtained simply by computing (7) for a choice of $M = L = N_s - 1$. Choosing $M = L$ in (6) yields a square linear system which has the important property of being circulant by construction. A circulant matrix is diagonalized by the DFT matrix and the computation of the (pseudo-)inverse becomes trivial by means of the Fast Fourier Transform.

Specifically, denoted with $\mathbf{F}$ the square $N_s \times N_s$ matrix with elements

$$F_{nm} = \frac{1}{\sqrt{N_s}} e^{-J2\pi \frac{nm}{N_s}}, \tag{10}$$

the following equality holds for our choice of the probing signal c_n:

$$\mathbf{F}^H \mathbf{X} \mathbf{F} = \sqrt{M}\,\mathrm{diag}(\mathbf{c}^*) e^{-J\pi(M-1)/4} \tag{11}$$

where the vector $\mathbf{c}$ is given by $\mathbf{c} = [c_0, c_1, \ldots, c_{M-1}]^T$.

Using this equality in the computation of (7) yields:

$$\hat{\mathbf{h}} = \left(\mathbf{X}^H \mathbf{X}\right)^{-1} \mathbf{X}^H \mathbf{y} = \frac{e^{J\pi(M-1)/4}}{\sqrt{M}} \mathbf{F}\,\mathrm{diag}(\mathbf{c}) \mathbf{F}^H \mathbf{y}. \tag{12}$$

This expression can be further simplified by observing that $\mathbf{Fc} = \mathbf{c}^* e^{J\pi(M-1)/4}$, which yields, after a few manipulations:

$$\hat{\mathbf{h}} = \frac{1}{\sqrt{M}} \mathrm{diag}(\mathbf{c}^*) \mathbf{F}^H (\mathrm{diag}(\mathbf{c}^*)\mathbf{y}). \tag{13}$$

This means that our choice of the sounding sequence yields an extremely low complexity channel estimation algorithm with can be performed in real-time with low-cost hardware (see section IV-E below for an analysis of the computational complexity).

The channel estimates we obtain every N_s samples are still affected by synchronization errors. The random time delay can be ignored since we are only interested in measuring the Delay Spread, while Carrier Frequency Offset(s) and the average Doppler caused by relative motion between transmitter and receiver can be compensated canceling the phase term of the direct path This phase term can be estimated by searching for phase of the estimated sample with maximum amplitude (which is the less affected by noise). Finally, clock drifts can be measured and compensated as described in [33].

D. CHANNEL SPREADING PARAMETER ESTIMATION

For evaluating the temporal variability of the channel impulse response, we repeat the estimation process for N_c repetitions of the sounding sequence. By analyzing the whole set of N_c channel estimates, the receiver can compute the channel spreading parameters we are looking for. The delay spread is estimated by finding the common smallest delay interval accounting for α_{DS} (typically the 95%) of the channel impulse response energy.

In order to estimate the Doppler spread, we first compute the channel frequency response (by means of an FFT) for each estimate of the N_c channel impulse responses. Then we compute the autocorrelation of each frequency sample, along the channel-estimate-index dimension, i.e. we obtain N_s autocorrelations each of $2N_c - 1$ points. Last, we compute the DFT of the average of these autocorrelations and obtain the Doppler Spectrum estimate. We use the obtained Doppler Spectrum estimate to measure the Doppler spread as half of the interval accounting for α_{BD} (again, typically 95%) of the overall power spectrum, i.e. we measure only positive frequencies.

E. COMPUTATIONAL COMPLEXITY ANALYSIS

The proposed method requires the estimation of the channel impulse response (by means of equation 13), which is based on the well-known FFT algorithm. Since the estimation is done on N_s samples and is repeated N_c times, the channel estimation mechanism described in § IV-C has computational complexity $O(N_c \cdot N_s log(N_s))$. Once the channel impulse response is measured, estimation of the Delay spread is trivial and does not increase the order of the complexity. To compute the Doppler spread as described in § IV-D, computation of the N_c channel frequency response measurements requires as

many FFTs on N_s points (same complexity as above), and the N_s autocorrelations of the frequency samples can also be computed by means of FFTs on $2N_c - 1$ points. However, since usually $N_s \gg N_c$, the overall computational complexity of the proposed method remains $O(N_c \cdot N_s log(N_s))$.

Note that, compared to other strategies which aim at estimating channel distortions on every single packet or even on every symbol (e.g. [6], [17]), the proposed method might be used only seldomly on stable channels (or whenever the channel undergoes significant changes), potentially reducing the time, frequency and power resources required for this purpose. Indeed, most of the power consumption is absorbed by the transducer in TX/RX mode, which is two or three orders of magnitude higher than Idle mode [29].

V. ANALYSIS OF EXEMPLARY UNDERWATER CHANNELS

In order to validate our technique for estimating the channel spreading parameters, we used two channel simulators: an in-house developed channel simulator which is similar to [34], and the well-known Watermark channel simulator [33]. Finally, we employ our channel estimation technique in two sea environments and analysed the feasibility (or not) of the OFDM modulation in different sites.

A. AD-HOC TIME-VARYING CHANNELS

We implemented a custom-made simulator for underwater channels, in which the time-varying channel responses can be specified in terms of number of reflected paths N_p, as well as per-path attenuation and temporal variability of the propagation delay. Although this channel specification can be somehow simplistic, it allows us to exactly model the channel responses over time and therefore refer to a ground truth for assessing the performance of channel spreading estimates.

More into details, the linear time-varying (LTV) model of the impulse response obey to the following equation:

$$h(t, \tau) = \sum_{p=1}^{N_p} \rho_p \delta(t - \tau - d_p(t)/c) \tag{14}$$

where N_p is the number of paths included in the multi-path channel response, and we chose, for simplicity, constant amplitudes ρ_p and a constant sound speed c. The functions $d(t)$ can be tweaked at will in order to model relative movements between the transmitter, the receiver, and the scattering sources.

A first model we considered, denoted by LTV1, uses $d_p(t)/c = \tau_{0,p} + \tau_{1,p} cos(\omega_p t + \phi_p)$. With this choice, it is possible to model the communication channel between users which are stationary on average, and affected by a sinusoidal time-varying wave movement. An argument similar to the evaluation of the bandwidth of a Frequency Modulated signal leads to the following approximation for the Doppler spread of such a channel: $\max_p[\omega_p(f_0\tau_{1,p} + 1/2\pi)]$, where f_0 is the center frequency of the transmitted signal. Conversely, the delay spread can be computed directly in terms of the τ_0 and τ_1 parameters.

TABLE 2. Simulation parameters of the LTV1 channel model with three main paths.

Variable	Value(s)
N_p	3
ρ^2	$[0.68, 0.24, 0.08]$
τ_0	$[1, 4, 15]$ (ms)
τ_1	1 (ms)
ω	0.06π
ϕ	$U(-\pi, \pi)$

In order to evaluate the impact of the α_{DS} and α_{BD} estimation parameters introduced in the previous section - respectively the Delay Spread and Doppler Spread truncation errors - we ran simulations of a coded OFDM modem over the LTV1 channel model with three main paths as reported in Table 2. The OFDM modulation is calibrated by using the design criteria of our intelligent module, i.e. by configuring $N_{CP} = DelaySpread/T_s$ and $N = 0.08/(DopplerSpread \cdot Ts) - N_{CP}$. Therefore, using the proposed channel estimation mechanism, the modem can measure the Delay and Doppler spread and tune the OFDM parameters automatically, by changing the number of subcarriers N and prefix length N_{CP}.

Figure 3(a) shows the Bit Error Rate performance of coded OFDM on the LTV1 channel and a noise-free scenario as a function of different truncation errors on the evaluation of Delay and Doppler spread values. The noise-free assumption allows to assess the impact of inter-symbol interference (ISI) and inter-carrier interference (ICI). Inspection of the figure shows that, in order to limit the effects of these two interference terms, it is necessary to select a high enough threshold (i.e. a low enough truncation error). However, if the choice of these parameters is too high (or in overspread scenarios), the constraints on the OFDM lead to an unfeasible modulation design. The choice of the α_{DS} and α_{BD} parameters thus depends both on the application scenario and the tolerable interference levels, and will be a function of the modulation and coding set.

B. WATERMARK CHANNELS

We applied our technique for estimating the channel spreading parameters to other underwater simulated channels, based on the recordings of real channel traces. In particular, we worked on the Watermark simulator, which provides several time-varying channel traces measured in different real sites. The at-sea measurements of the channel impulse response were performed using linear frequency modulated signals (chirps) or spectrally-white pseudo-noise input sequences. The idea of recording real channel traces was motivated by the need of providing a benchmark for physical-layer algorithms under realistic and reproducible conditions.

More into details, watermark is issued with a library of channels measured in Norway (two sites), France, and

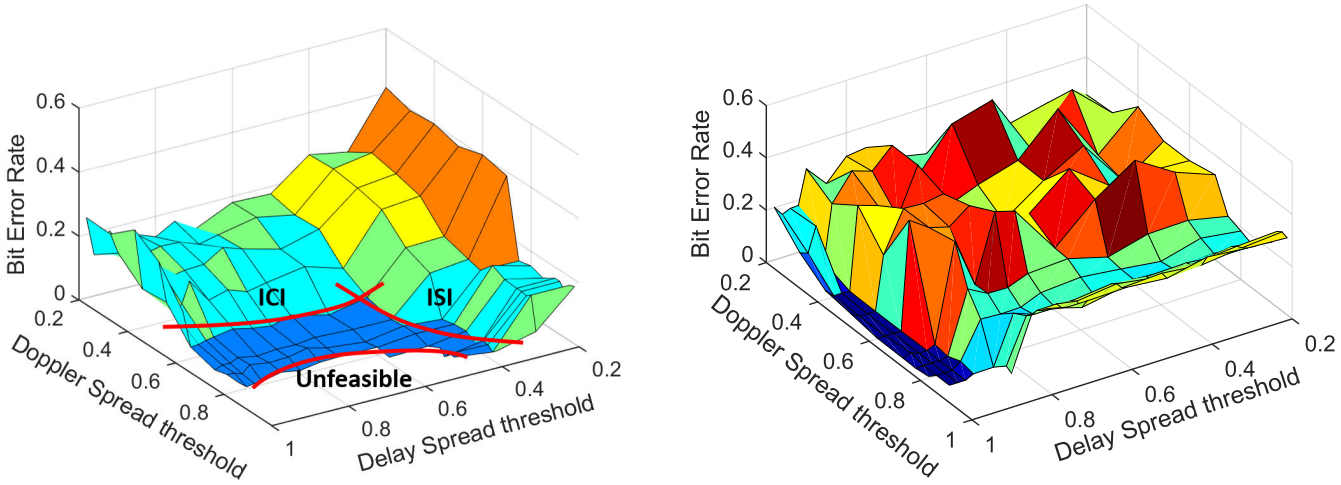

FIGURE 3. Bit Error Rate performance of coded OFDM with decision feedback on the LTV1 and NOF1 channels, as a function of the delay and Doppler spread estimation thresholds.

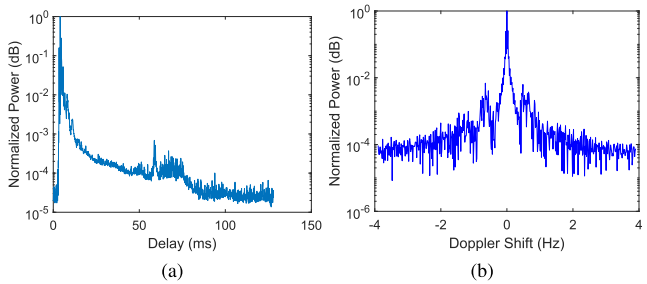

FIGURE 4. Impulse response and Doppler spectrum for a sample sounding of Watermark channel NOF.

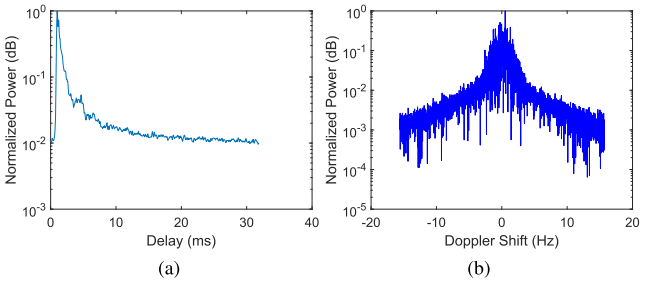

FIGURE 5. Impulse response and Doppler spectrum for a sample sounding of Watermark channel NCS.

Hawaii, offering three frequency bands (4–8, 10–18, and 32.5–37.5 kHz), single-hydrophone and array receivers, and play times varying from 33 seconds to 33 minutes. The Watermark channels come in two varieties, single-input single-output (SISO) and single-input multiple-output (SIMO). In our experiments, we used the available SISO channels since most acoustic modems use a single receiver.

We analysed the channel characteristics of Watermark's NOF1 and NCS1 traces, which both have 8 kHz bandwidth in the range 10-18 kHz and are measured between two stationary nodes. In particular, the NOF1 dataset is constituted of 60 different soundings recorded in a shallow stretch of water, with a total play time of about 33 min. Each of the 60 soundings is long 32.9 s and was measured transmitting 258 consecutive chirps signals lasting 128 ms (2048 samples at 16 kHz sampling rate). For example, Fig. 4 reports one channel impulse response and the Doppler spectrum measured for one of these 60 soundings. Across the entire dataset, the estimated Delay spread (considering 95% of the impulse response energy) ranged between 10 and 80 ms and the Doppler spread $\in$ [0.6, 2.2] Hz.

The NCS1 dataset is also constituted by 60 different soundings but measured on Norway's continental shelf using pseudonoise sequences. Each measurement is 32.6 seconds long, consisting of 1024 probing sequences 31.9 ms long (510 samples at 16 kHz sampling rate), yielding a total play time of almost 33 minutes. As reported in [33], NCS1 is more challenging than NOF1, because the true channel is characterized by long delay and Doppler tails, which are aliased in the measurement (although the fraction of energy that is aliased is not necessarily large). For example, Fig. 5 shows the channel impulse response and Doppler spectrum of a sample sounding. Across the entire dataset, the estimated Delay spread was around 31.6 ms (close to the measurement limit) and the Doppler spread was between 8.7 and 10.7 Hz. The NCS1 channel is thus an interesting representative test for harsh environments.

Figure 3(b) shows the Bit Error Rate performance of coded OFDM, designed according to our intelligent module, on the NOF1 channel. Again, inspection of the figure shows that, in order to obtain a good BER performance, it is necessary to choose a relatively high threshold α_{DS} for Delay Spread estimation (over 90%), while a relatively low threshold α_{BD} is sufficient (not lower than 40%). The figure for

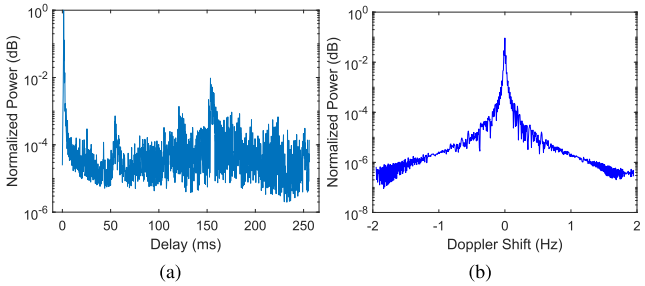

FIGURE 6. Impulse response and Doppler spectrum at sea using 258 chirps.

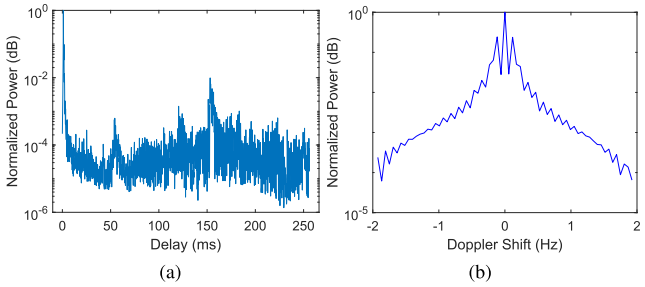

FIGURE 7. Impulse response and Doppler spectrum at sea using only 34 chirps.

the NCS1 channel instead is not shown, as OFDM either had a high BER (when using low thresholds which led to high interference), or resulted unfeasible. As we will show, the fall-back modulation can be successfully used in such scenarios.

C. SEA CHANNELS EXPERIMENTS

Finally, we tested the proposed estimation technique at sea in a touristic harbor at Santa Marinella, close to Rome, Italy, in three different settings (see more details in sec. VI-B). Similar to Watermark probing signals, for the measurements we employ trains of 258 consecutive chirps. We tested different chirp durations of 64, 128 and 256 ms and varied the root-raised-cosine filter length between 6 and 48 samples (with steps of 6 samples). For example, Fig. 6 shows the channel impulse response and Doppler spectrum measured on one of these measurements. Overall, the estimated Delay spread (considering 95% of the energy) varied widely between 1.3 and 79 ms, while the Doppler spread was always between 0.5 and 1.5 Hz.

While such measurements lead to accurate estimates of the channel parameters, they require up to over one minute to be accomplished. In practice, in less harsh environments (i.e. when the channel allows the use of OFDM modulation) it is often possible to reduce this measurement time, employing shorter chirp trains and accepting a more coarse Doppler estimation. For example, Fig. 7 shows the results obtained in one of the experiments using only 34 chirps. In this scenario, while the corresponding Delay spread is not seriously affected, the Doppler spread measurement is affected by a loss in resolution with an increase in the estimation. This can be partially compensated by lowering the Doppler threshold or, for harsher scenarios, increasing again the number of estimates.

TABLE 3. Design of OFDM parameters for tested channels.

Channel	Delay sp. (ms)	Doppler sp. (Hz)	N	N_{CP}
NOF1	13.5	0.6	128	90
NCS1	31.6	8.6	–	–
Harbor Link 1	19.8	0.9	512	260
Harbor Link 2	44.2	0.5	1024	576
Harbor Link 3	65.8	1.3	–	–

Table 3 summarizes the (average) channel parameters obtained and the corresponding minimum cyclic prefix length N_{CP} and maximum number of subcarriers N according to the OFDM constraints described in sec. III-B. From the table, it is clear that high performance OFDM can be obtained in most of the Harbor links (more details in sec. VI-B), while it is not possible to use OFDM on the NCS channel.

VI. OFDM MODULATOR PERFORMANCE

We tested the performance of our OFDM modulator in simulated and real channels, under different configurations of the number of sub-carriers N and prefix length N_{CP}. In particular, we varied the number of sub-carriers from a minimum of 64 to a maximum of 256 (in power of 2) and the cyclic prefix in the range from 30 to 110 samples (never exceeding the number of subcarriers). We set the length of the OFDM packet to 4, 8, 16 or 32 symbols which, depending on the parameters and modulation used, can carry from few hundred bytes to a few kilobytes. The bits to be transmitted are generated randomly, consistently with the number of OFDM symbols chosen, and we apply a convolutional coding with rate equal to 1/2 to the data (i.e. only half of the bits are information, while the rest are redundancy bits generated by the convolutional code). The bits are then mapped using a QPSK constellation to the various data subcarriers.

A. EXPERIMENTS WITH SIMULATED CHANNELS

The analysis of simulated channels is based on the Watermark simulator using the NOF1 dataset. We varied different modulation parameters and, for each experiment, we transmit at least 100 packets on each sounding, collecting thousands of channel traces in total. We show here a subset of the results for the sake of brevity. In the experiments, we also added an increasing level of AWGN noise, with a residual Signal-to-Noise Ratio (SNR) from 40 dB down to 10 dB. We emphasize, however, that the SNR level shown is not an absolute limit of the modulation, since the AWGN noise is added to the signal already affected by the NOF1 channel (which is noisy by itself).

Fig. 8 shows the BER obtained in Watermark's NOF1 channel using packets of 16 symbols, $N = 128$ subcarriers, cyclic prefix length $N_{CP} = 70$, $\alpha_p = 0.2$ and $L_p = 6$. Note that $N_{CP} = 70$ is slightly below the ISI

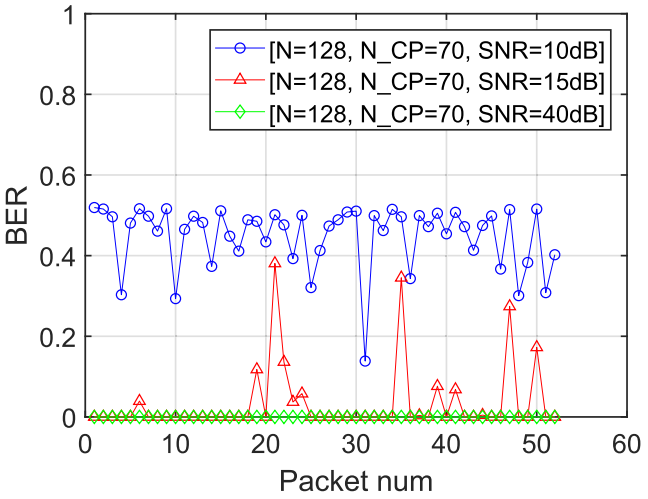

FIGURE 8. OFDM results in Watermark's NOF1 channel with a packet length of 16 symbols and various levels of AWGN noise.

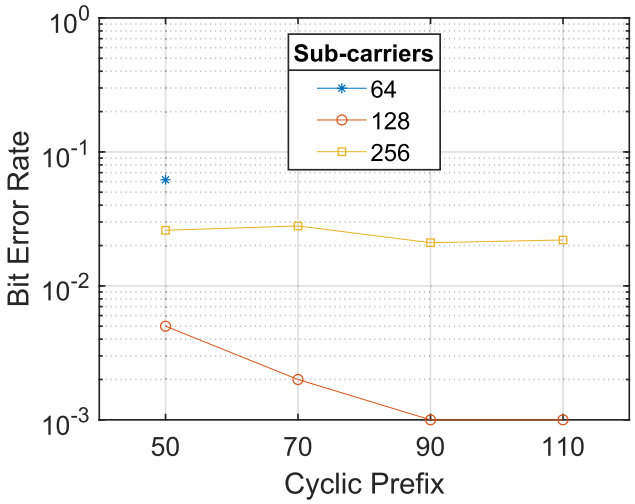

FIGURE 9. Experiments with Watermark channel NOF1: impact of the OFDM cyclic prefix length with different number of subcarriers and packet length of 32 symbols.

limit, but the receiver still works if the SNR is high enough (SNR = 40 dB). Indeed, in this case despite the underwater channel is affecting the signal, the proposed receiver is able to correctly demodulate the without any error (BER = 0). However, if the SNR decreases, the proposed decision-feedback receiver will suffer from error propagation: indeed, the channel estimates used for detection are corrupted by channel noise, and poor estimates lead to high error rates which in turn cause a failure of subsequent channel estimates. This is evident for the 10 dB example shown in figure 8(a), and improves with higher SNR ratios. Nevertheless, increasing the cyclic prefix length to 90 samples is sufficient to get reliable performance even with packets that are 32 symbols long, as shown in Fig. 9.

We also tested the impact of other modulation parameters. Regarding the root-raised cosine filter, we vary the roll-off factor α_p to be equal to 0.15, 0.2 and 0.25, while the filter length L_p varies from 6 to 12 (in steps of 3). The roll-off factor α_p defines the excess bandwidth used compared to a pulse with a rectangular spectrum of equal bandwidth. Smaller roll-off values result in higher spectral efficiency, as more sub-carriers can be used for data, but requires longer filtering delays (i.e. higher L_p). The results obtained changing the α_p and L_p parameters of the filter are omitted since have less impact compared to N and N_{CP}.

B. EXPERIMENTS AT SEA

We confirm the OFDM results obtained in Watermark by repeating the experiments at sea in a touristic harbor at Santa Marinella, close to Rome, Italy. We tested three different settings (which we refer to as Link 1, Link 2, Link 3), where we placed the transmitter and the receiver as shown in Fig. 10: for Link 1, we set the modems approximately 30 m apart, between to two floating docks; for Link 2, the modems are at 200 m distance, across the entire harbor; finally, Link 3 is approximately 140 m long and traverses the entrance of the

FIGURE 10. Experimental setup in a touristic harbor in Santa Marinella, close to Rome, Italy.

harbor. The water depth was 3 m and the transducers were placed about 1 m below sea level. For these experiments we used the EvoLogics S2C 18/34 transducers, controlled in SDM mode.

Since the transducers have a bandwidth of 16 kHz (twice as much as the NOF1 Watermark channel), we also increased the range of OFDM parameters to be tested: we vary the number of subcarriers from 256 up to 1024 and the length of the cyclic prefix up to 240 samples (never exceeding the number of subcarriers). We vary the length of the packets between 4 and 32 symbols and the α_p and L_p parameters in the range [0.15 – 0.25] and [6 – 9] respectively. Note that, as reported in sec. V-C, on Link 3 the channel parameters do not allow the use of OFDM, so in this scenario the fall-back modulation is activated by the intelligent module.

For the Link 1 scenario, in a worst case scenario employing 32 symbols packets, Fig. 11 shows that with low Doppler shifts, good performance can be obtained even with

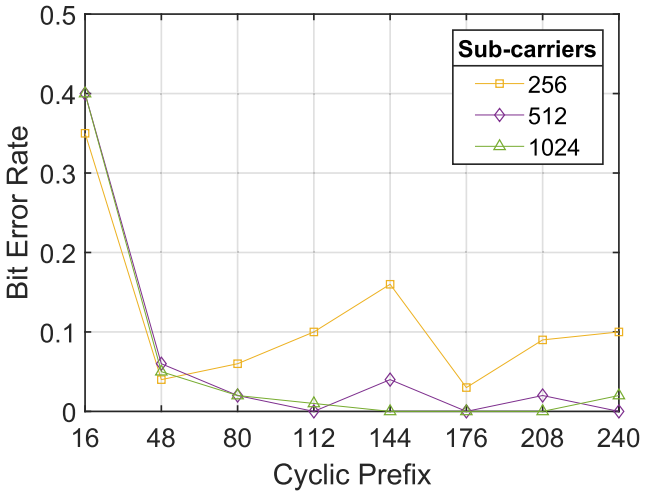

FIGURE 11. Experiments on harbour Link 1: average BER for coded OFDM with 32 symbols packets as a function of N_{CP} and different number of sub-carriers.

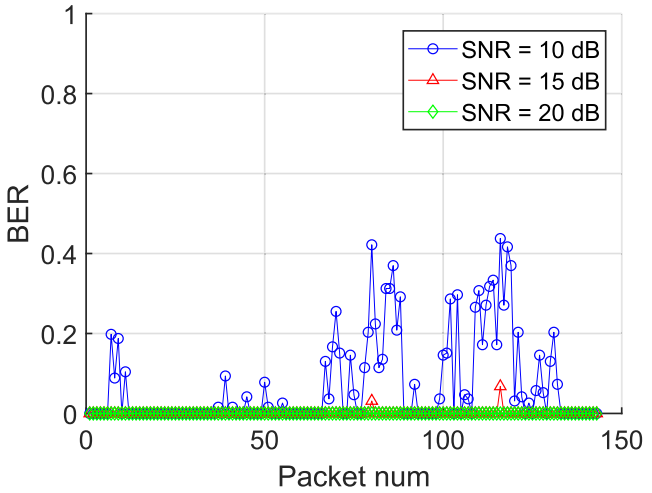

FIGURE 12. JANUS results under the Watermark NCS1 channel in different SNR conditions.

1024 subcarriers and N_{CP} lower than 250, with a BER lower than 5% even with 32 OFDM symbols long packets. Similar results were obtained on Link 2, where the BER was even lower (about 1%). In terms of data rate, the proposed modem achieved a spectral efficiency of 1.25 bit/s/Hz (corresponding to 20 kbit/s using QPSK), which is in line with the results of [2], although the BER is slightly higher due to the harsher experimental environment.

VII. FALL-BACK MODULATOR PERFORMANCE

Finally, we validated the fall-back modulator performance in harsh channel conditions, when the OFDM modulator does not work or exhibits very poor performance. We used Watermark's NCS1 channel which was shown unfeasible for every possible combination of OFDM parameters. This modulation was also used at sea (Harbor Link 3) since in this scenario strong currents may appear because of the tides. In these cases, the intelligent module can detect such conditions and activate the fall-back modulation.

The modulation of choice for harsh environments, is the binary FSK with frequency hopping used by the JANUS modulator. Indeed, the FSK modulation allows a very simple implementation of transmitter and receiver operations and the frequency hopping allows to skip the interference created by the signal reflections in the frequency domain, thus allowing a higher rate at the expense of spectral efficiency. Demodulation is performed by following the pre-defined hopping sequence, by differentiating the instantaneous received frequency and running the matched filter.

As described previously, Watermark NCS1 is a challenging scenario, with long Delay spread (higher than 30ms) and Doppler spread higher than 8Hz, which are subject to measurement aliasing (as reported in [33]). We also simulated the effect of an additive AWGN noise, with a tunable power, leading to a residual Signal-to-Noise Ratio (SNR) ranging from 10 dB to 20 dB.

Figure 12 shows the BER obtained by our JANUS implementation slightly modified to adapt to the NCS1 channel. From the figure, it is clear that the Fall-back modulation is free from errors when the residual SNR is above 15-20 dB (BER $= 0$). We also exploited our software-based implementation for removing the frequency hopping mechanism. In this case, the BER was close to 0.5 for all the simulated packets and SNR values. Indeed, the JANUS symbol lasts 6.26 ms, which is much lower than the Delay Spread of the NCS channel (31.6 ms). The frequency hopping strategy is thus essential on this channel, despite the other Doppler correction and Trellis code mechanisms implemented in JANUS for robust demodulation. Excellent results were also obtained in the Harbor Link 3, which we omit for the sake of brevity.

VIII. CONCLUSION

In this work we designed a channel-aware adaptive modem based on a low-cost software-defined architecture. In particular, we devised a simple strategy to exploit high rate OFDM communications (when the channel allows it) and dynamically adjust the parameters to cope with the expected Doppler shift and multipath delay. Contrary to previous approaches, which tailor particular environments or employ complex Doppler correction techniques, we proposed a low-complexity estimation technique for time-varying channels and an intelligent module for tuning the OFDM parameters as a function of the channel spreading estimates. The proposed approach has been validated in different simulation platforms for underwater communications and in real experiments at sea, representing a variety of harsh and mild scenarios. Results show that OFDM achieves good performance in the latter conditions, while a fall-back modulation can be used in the former. Finally, our SDAM can be extended with different modulations (S2C, hybrid-carrier), thus increasing the possibility to adapt to the various underwater scenarios, which this is left for future work.

REFERENCES

[1] M. Stojanovic and J. Preisig, "Underwater acoustic communication channels: Propagation models and statistical characterization," *IEEE Commun. Mag.*, vol. 47, no. 1, pp. 84–89, Jan. 2009, doi: 10.1109/MCOM.2009.4752682.
[2] E. Demirors, G. Sklivanitis, G. E. Santagati, T. Melodia, and S. N. Batalama, "A high-rate software-defined underwater acoustic modem with real-time adaptation capabilities," *IEEE Access*, vol. 6, pp. 18602–18615, 2018, doi: 10.1109/ACCESS.2018.2815026.
[3] J. Potter, J. Alves, D. Green, G. Zappa, I. Nissen, and K. McCoy, "The JANUS underwater communications standard," in *Proc. Underwater Commun. Netw. (UComms)*, Sestri Levante, Italy, Sep. 2014, pp. 1–4.
[4] K. G. Kebkal and R. Bannasch, "Sweep-spread carrier for underwater communication over acoustic channels with strong multipath propagation," *J. Acoust. Soc. Amer.*, vol. 112, no. 5, pp. 2043–2052, Nov. 2002.
[5] C. Baldone, G. E. Galioto, D. Croce, I. Tinnirello, and C. Petrioli, "Doppler estimation and correction for JANUS underwater communications," in *Proc. IEEE Global Commun. Conf. (GLOBECOM)*, 2020, pp. 1–6, doi: 10.1109/GLOBECOM42002.2020.9348220.
[6] N. Parrish, S. Roy, and P. Arabshahi, "Symbol by symbol Doppler rate estimation for highly mobile underwater OFDM," in *Proc. 4th ACM Int. Workshop UnderWater Netw. (WUWNet)*, Berkeley, CA, USA, Nov. 2009, pp. 1–8.
[7] G. E. Galioto, D. Garlisi, D. Croce, L. Mistretta, R. Badalamenti, I. Tinnirello, C. G. Giaconia, C. Petrioli, and P. Gjanci, "FLUMO: FLexible underwater MOdem," in *Proc. OCEANS*, Marseille, France, Jun. 2019, pp. 1–7.
[8] M. Stojanovic and L. Freitag, "Recent trends in underwater acoustic communications," *Marine Technol. Soc. J.*, vol. 47, no. 5, pp. 45–50, 2013, doi: 10.4031/MTSJ.47.5.9.
[9] M. Stojanovic, "Low complexity OFDM detector for underwater acoustic channels," in *Proc. OCEANS*, 2006, pp. 1–6, doi: 10.1109/OCEANS.2006.307057.
[10] A. Radosevic, R. Ahmed, T. M. Duman, J. G. Proakis, and M. Stojanovic, "Adaptive OFDM modulation for underwater acoustic communications: Design considerations and experimental results," *IEEE J. Ocean. Eng.*, vol. 39, no. 2, pp. 357–370, Apr. 2014.
[11] P. J. Gendron, "Orthogonal frequency division multiplexing with on-off-keying: Noncoherent performance bounds, receiver design and experimental results," *U.S. Navy J. Underwater Acoust.*, vol. 56, no. 2, pp. 267–300, Apr. 2006. April 2014, doi: 10.1109/JOE.2013.2253212.
[12] L. Wan, H. Zhou, X. Xu, Y. Huang, S. Zhou, Z. Shi, and J.-H. Cui, "Adaptive modulation and coding for underwater acoustic OFDM," *IEEE J. Ocean. Eng.*, vol. 40, no. 2, pp. 327–336, Apr. 2015.
[13] B. Li, S. Zhou, M. Stojanovic, L. Freitag, and P. Willett, "Non-uniform Doppler compensation for zero-padded OFDM over fast-varying underwater acoustic channels," in *Proc. OCEANS Europe*, Jun. 2007, pp. 1–6.
[14] S. Mason, C. Berger, S. Zhou, and P. Willett, "Detection, synchronization, and Doppler scale estimation with multicarrier waveforms in underwater acoustic communication," *IEEE J. Sel. Areas Commun.*, vol. 26, no. 9, pp. 1638–1649, Dec. 2008.
[15] C. Baldone, G. E. Galioto, D. Croce, I. Tinnirello, and C. Petrioli, "Doppler estimation and correction in underwater industrial Internet of Things," in *Proc. Int. Symp. Wireless Technol., Signal Process. Algorithms Meas. Techn. Ind. Internet Things (IMEKO TC)*, Palermo, Italy, 2020, pp. 174–178.
[16] T. Arikan, T. Riedl, A. Singer, and J. Younce, "Comparison of OFDM and single-carrier schemes for Doppler tolerant acoustic communications," in *Proc. OCEANS Genova*, Genova, Italy, May 2015, pp. 1–7.
[17] J. Li, Y. V. Zakharov, and B. Henson, "Multibranch autocorrelation method for Doppler estimation in underwater acoustic channels," *IEEE J. Ocean. Eng.*, vol. 43, no. 4, pp. 1099–1113, Oct. 2018, doi: 10.1109/JOE.2017.2761478.
[18] (2016). *Evologics Underwater Acoustic Modems*. [Online]. Available: https://www.evologics.de
[19] M. Chitre, I. Topor, and T. Koay, "The UNET-2 modem—An extensible tool for underwater networking research," in *Proc. Oceans-Yeosu*, 2012, pp. 1–7, doi: 10.1109/OCEANS-Yeosu.2012.6263431.
[20] *EvoLogics SDM Mode*. Accessed: May 21, 2021. [Online]. Available: http://github.com/EvoLogics/sdmsh
[21] *UNetStack*. Accessed: May 21, 2021. [Online]. Available: http://www.unetstack.net
[22] H. S. Dol, P. Casari, T. van der Zwan, and R. Otnes, "Software-defined underwater acoustic modems: Historical review and the NILUS approach," *IEEE J. Ocean. Eng.*, vol. 42, no. 3, pp. 722–737, Jul. 2017, doi: 10.1109/JOE.2016.2598412.
[23] B. Li, J. Huang, S. Zhou, K. Ball, M. Stojanovic, L. Freitag, and P. Willett, "MIMO-OFDM for high-rate underwater acoustic communications," *IEEE J. Ocean. Eng.*, vol. 34, no. 4, pp. 634–644, Oct. 2009.
[24] S. Shahabudeen, M. Chitre, M. Motani, and A. L. Y. Siah, "Unified simulation and implementation software framework for underwater MAC protocol development," in *Proc. OCEANS*, 2009, pp. 1–9, doi: 10.23919/OCEANS.2009.5422101.
[25] L. Freitag, M. Grund, S. Singh, J. Partan, P. Koski, and K. Ball, "The WHOI micro-modem: An acoustic communications and navigation system for multiple platforms," in *Proc. OCEANS MTS/IEEE*, vol. 2, 2005, pp. 1086–1092, doi: 10.1109/OCEANS.2005.1639901.
[26] E. Gallimore, J. Partan, I. Vaughn, S. Singh, J. Shusta, and L. Freitag, "The WHOI micromodem-2: A scalable system for acoustic communications and networking," in *Proc. OCEANS MTS/IEEE SEATTLE*, 2010, pp. 1–7, doi: 10.1109/OCEANS.2010.5664354.
[27] G. Cario, A. Casavola, M. Lupia, and C. Rosace, "SeaModem: A low-cost underwater acoustic modem for shallow water communication," in *Proc. OCEANS-Genova*, 2015, pp. 1–6, doi: 10.1109/OCEANS-Genova.2015.7271721.
[28] R. Petroccia, G. Cario, M. Lupia, V. Djapic, and C. Petrioli, "First in-field experiments with a 'bilingual' underwater acoustic modem supporting the JANUS standard," in *Proc. OCEANS Genova*, 2015, pp. 1–7, doi: 10.1109/OCEANS-Genova.2015.7271740.
[29] S. Sendra, J. Lloret, J. M. Jimenez, and L. Parra, "Underwater acoustic modems," *IEEE Sensors J.*, vol. 16, no. 11, pp. 4063–4071, Jun. 2016, doi: 10.1109/JSEN.2015.2434890.
[30] J. D. Gaedder. *Liquid, Software-Defined Radio Digital Signal Processing Library User's Manual*. Accessed: May 21, 2021. [Online]. Available: http://www.liquidsdr.org/downloads/liquid-dsp-1.2.0.pdf and http://liquidsdr.org/doc/fec/
[31] G. Garbo and S. Mangione, "An improved receiver architecture for cyclic-prefixed OFDM," in *Proc. IEEE Wireless Commun. Netw. Conf.*, Budapest, Hungary, Apr. 2009, pp. 1–6.
[32] J. Alves, T. Furfaro, K. LePage, A. Munafo, K. Pelekanakis, R. Petroccia, and G. Zappa, "Moving JANUS forward: A look into the future of underwater communications interoperability," in *Proc. OCEANS MTS/IEEE Monterey*, Monterey, CA, USA, Sep. 2016, pp. 1–6, doi: 10.1109/OCEANS.2016.7761094.
[33] P. A. van Walree, F.-X. Socheleau, R. Otnes, and T. Jenserud, "The watermark benchmark for underwater acoustic modulation schemes," *IEEE Journal of Oceanic Engineering*, vol. 42, no. 4, pp. 1007–1018, May 2017.
[34] B. Henson, J. Li, Y. V. Zakharov, and C. Liu, "Waymark baseband underwater acoustic propagation model," in *Proc. Underwater Commun. Netw. (UComms)*, Sep. 2014, pp. 1–5, doi: 10.1109/UComms.2014.7017132.

STEFANO MANGIONE (Member, IEEE) received the degree *(cum laude)* in electronics engineering and telecommunications curriculum, in 2000. He is currently an Assistant Professor in telecommunications engineering with the University of Palermo. Recently, his activities include automatic methods for registration of nuclear magnetic resonance images, multiuser receiver strategies for LoRa, and the study of underwater communication systems. His research interest includes physical layer aspects of communication systems, from forward error correction coding to equalization strategies for spread spectrum systems.

GIOVANNI ETTORE GALIOTO received the Laurea degree in telecommunication engineering from the University of Palermo, in 2014, where he is currently pursuing the Ph.D. degree with the ICT Program, under the supervision of Prof. I. Tinnirello, in collaboration with WSense srl.

DANIELE CROCE received the double M.Sc. degree in networking engineering from the Politecnico di Torino, Turin, Italy, and the EURECOM Institute, France, in 2006, the Diploma in Research Master (DEA) degree in networking and distributed systems from the Université de Nice-Sophia Antipolis (UNSA), Nice, France, in 2006, and the joint Ph.D. degree from the Politecnico di Torino and UNSA, in 2010. He is currently an Assistant Professor with the University of Palermo, Italy. He has a long experience of research collaborations in several European and national research projects on wireless networks, the Internet of Things, high-quality TV streaming, smart grid communications, and smart cities. He also worked on assistive technologies for visually impaired people. With the Arianna Project, he co-founded the start-up company In.sight srl, spin-off of Palermo University.

ILENIA TINNIRELLO received the Ph.D. degree in telecommunications engineering from the University of Palermo, in 2004. She was a Visiting Researcher with Seoul National University, South Korea, in 2004, and the Nanyang Technological University, Singapore, in 2006. She is currently a Full Professor with the University of Palermo. Recently, she is also working on the definition of novel services (smart grid, smart metering, and indoor localization) enabled by the pervasive availability of ICT technologies. She has been involved in several European research projects, among which the FP7 FLAVIA Project, with the role of a Technical Coordinator, and the H2020 WiSHFUL and Flex5Gware projects. Her research interest includes wireless networks, in particular on the design and prototyping of protocols and architectures for emerging reconfigurable wireless networks.

CHIARA PETRIOLI (Fellow, IEEE) is currently a Professor of computer science and the Director of the Sensor Networks and Embedded Systems Laboratory (SENSES Lab), Department of Computer Science, University of Rome La Sapienza. She is also leading the Cyber Physical System Laboratory, La Sapienza Center for Cyber Intelligence and Information Security, and a Founding Partner of La Sapienza spinoff WSense Srl. She has been a member of the Academic Senate and the Chair of the Ph.D. Program in computer science with La Sapienza. She is also a pioneer of the Internet of Underwater Things, an area on which she has led the development of breakthrough technologies listed in the NT100 Top Social Global Techs Changing Our Lives 2016. She has published over 150 articles in prominent international journals and conferences (over 6500 citations and H-index 45). She has been a PI of over 20 national and international research projects, serving as a coordinator of three EC projects (FP7 projects GENESI and SUNRISE, and EASME ArcheoSub) highlighted as success stories on the Digital Agenda of Europe and featured by international mass media, including RAI SuperQuark and Presa Diretta, Wired USA, The Guardian, Bild Magazine, and National Geographics. Her research has resulted in international patents and in award-winning innovative technologies. Her research interests include the design and optimization of future wireless, embedded, the IoT, and cyber physical systems. She has been a member of the Steering Committee of ACM SenSys, the Executive Committee of ACM SIGMOBILE, and the ACM Europe Council. She is also a Fulbright Scholar, one of the Inspiring 50 2018, the Top Women in Technology, and the Top Women of the N2Women 2019 Stars in computer networking and communications. She has been a member of the Steering Committee and an Associate Editor of IEEE TRANSACTIONS ON MOBILE COMPUTING, an Associate Editor of IEEE TRANSACTIONS ON VEHICULAR TECHNOLOGY and *Computer Communications* (Elsevier), and a Guest Editor of special issues for IEEE ACCESS, *Ad Hoc Networks* (Elsevier), and *Physical Communication* (Elsevier). She was the General Chair of ACM SenSys 2013 and the Program Co-Chair of IEEE INFOCOM 2016. She is also the Chair of the Steering Committee of IEEE SECON and the General Chair of ACM MobiHoc 2019. She has been the Program Co-Chair of leading conferences in the field, such as ACM MobiCom and IEEE SECON.